

Rafael Kurtz · Thomas Schirm · Harald Jockusch

## Maturation and myotonia influence the abundance of cation channels $K_{DR}$ , $K_{IR}$ and $C_{IR}$ differently: a patch-clamp study on mouse interosseus muscle fibres

Received: 2 February 1999 / Received after revision: 27 April 1999 / Accepted: 7 May 1999 / Published online: 22 June 1999

**Abstract** To detect cation channels, the expression of which is dependent on the physiological state of muscle, single-channel activities of dissociated fibres of the mouse interosseus muscle were recorded using the patch-clamp technique in the cell-attached mode. Fibres were prepared from juvenile and adult wild-type (WT), from chloride channel-deficient myotonic and from denervated adult WT muscles. In all cases delayed-rectifier  $K^+$  channels ( $K_{DR}$ ) with a unitary conductance of 11 pS were recorded in more than 95% of sarcolemmal patches, but with a low, steady-state open probability. Inwards-rectifying  $K^+$  channels ( $K_{IR}$ ) with a conductance of 31 pS in 140 mM  $[K^+]_o$  were active in about 50% of the membrane patches from WT and in more than 90% of those from myotonic fibres. A hitherto undescribed, inwards-rectifying, cation channel, provisionally termed  $C_{IR}$ , with fast kinetics and a unitary conductance of 36 pS, was active in nearly every membrane patch from juvenile mice, both WT and myotonic. The abundance of  $C_{IR}$  decreased during development, but was not changed 7 days after denervation of adult WT muscle.  $Ca^{2+}$ -dependent  $K^+$  channels were seen sporadically. Channels with the characteristics of adenosine 5'-triphosphate (ATP)-sensitive  $K^+$  channels were recorded frequently upon excision of membrane patches, but remained inactive in most cell-attached recordings. In conclusion, of the investigated ion channels, only  $K_{IR}$  was responsive to the activity pattern of adult muscle, whereas  $C_{IR}$  was down-regulated during muscle maturation.

**Key words** Skeletal muscle fibre · Cation channel · Inwards rectifying  $K^+$  channel ·  $K^+$  conductance · Development · Myotonia · Hyperexcitability · Denervation

### Introduction

A large, and still growing, number of  $K^+$  channel genes is presently being characterized by molecular cloning methods combined with expression studies in manipulated heterologous cells such as complementary ribonucleic acid (cRNA)-injected frog oocytes or complementary deoxyribonucleic acid (cDNA)-transfected tissue culture cells. On the other hand, the role of  $K^+$  currents in excitable cells has been studied by electrophysiological recordings combined with pharmacological blockade and overall changes of plasmalemmal  $K^+$  conductance during differentiation and maturation of muscle fibres have been observed [9, 12]. The excitability of the sarcolemma is governed by chloride and cation channels, the expression of which is, in part, dependent on the excitation pattern. The expression of these channels may thus be a link in a long-term regulatory feedback loop. However, the correlation between single-channel characteristics as determined by patch-clamp studies of cells expressing the ion channel under investigation naturally and the corresponding genes and their pattern of regulation is still rather incomplete for voltage-gated cation channels in general and  $K^+$  channels in particular. The complex population of these channels as predicted from their genetic diversity [17, 37], their variable physiological characteristics due to combination with accessory subunits and modulating mechanisms [3] and the scarcity of useful and specific blocking agents for these channels has hampered progress.

In the present study we addressed this problem for skeletal muscle by using the near-native preparation of dissociated mature muscle fibres and by studying the abundance of several voltage-gated cation channels as a function of developmental and physiological variables, namely age, hyperexcitability due to a lack of chloride

R. Kurtz · T. Schirm · H. Jockusch (✉)  
Entwicklungsbiologie und molekulare Pathologie,  
Universität Bielefeld, D-33501 Bielefeld, Germany  
e-mail: h.jockusch@biologie.uni-bielefeld.de  
Tel.: +49-521-1065618  
Fax: +49-521-1065654

*Present address:*

R. Kurtz, Abteilung für Neurobiologie, Universität Bielefeld,  
D-33501 Bielefeld, Germany

conductance, and denervation. Our investigation was concerned particularly with the following peculiarities of sarcolemmal  $K^+$  conductance in mammalian skeletal muscle ( $G_K$ ). First, during postnatal development in rats,  $G_K$  decreases whereas  $G_{Cl}$  increases [9]. Second, in the myotonic mouse mutant ADR ("arrested development of righting response"), lowered  $G_{Cl}$  values, responsible for muscle hyperexcitability, are accompanied by a reduction of  $G_K$  to less than half [7]. Third, whole-cell, inwards-rectifying  $K^+$  currents ( $K_{IR}$ ), thought to contribute to resting  $G_K$ , are up-regulated postnatally in mouse muscle. This increase is reversed by denervation [12].

It is not known whether these changes simultaneously affect the many types of  $K^+$  channels contributing to resting conductance or only one or a few kinds specifically. Recently,  $K_v3.4$  messenger RNA (mRNA) levels have been shown to be lowered by myotonic hyperexcitability [36]. This finding, however, can hardly account for the lowered  $G_K$  of myotonic muscle, since  $K_v3.4$  is an A-type  $K^+$  channel that probably does not contribute significantly to resting  $G_K$ . We therefore investigated, on the single-channel level, which  $K^+$ -permeable ion channels are active near resting membrane potential (RMP), and whether the abundance of these channels is regulated by muscle activity. We used cell-attached recordings from isolated muscle fibres to be able to estimate the contribution to total conductance at RMP of different channels under close to in situ conditions, i.e. with intracellular regulation mechanisms intact. A preliminary report of parts of this work has appeared in abstract form [22].

## Materials and methods

### Mice

Both wild-type (WT) mice and mice homozygous for the mutated allele *Clc1<sup>adr</sup>*, rendering the gene *Clc1* for the muscular  $Cl^-$  channel non-functional [25, 32] (myotonic, ADR mice), were bred in our laboratory on the original A2G background (c.f. [13]). Hind-limb muscles were denervated in 68- to 70-day-old, pentobarbitone sodium (Nembutal, 72 ng/g for males, 90 ng/g for females, injected i.p. as a 6 mg/ml solution in saline)-anaesthetized mice by transecting the sciatic nerve of one leg. In some cases, the effect of denervation was validated by Northern blot analysis of nicotinic acetylcholine receptor- $\alpha$  subunit (nAChR $\alpha$ ) expression, which is steeply up-regulated upon denervation (see [29]).

### Preparation of muscles and fibres

The interosseus muscle was dissected from the hind-limbs of freshly killed mice. Single muscle fibres were obtained by incubating interosseus muscles in Dulbecco's modified Eagle's medium (DMEM) containing 2 mg/ml collagenase (Gibco, Eggenstein, Germany) and 1 mg/ml protease (type IX, Sigma, Deisenhofen, Germany) in a rotary shaker at 36 °C. Enzymatic digestion was stopped when single fibres were seen to detach from the tissue (varying from 60 min for muscles from young mice and 90 min for those from adult mice) and fibres were completely dissociated by gentle trituration through a pipette tip. Fibres were maintained under tissue culture conditions in DMEM containing 10% FCS for at least 2 h and used for measurements within the next 2 days.

Denervation under pentobarbitone anaesthesia and killing by gradually increasing  $CO_2$  concentration were performed according to the German law for the protection of animals with a permit from the appropriate authorities.

### Recording methods.

The patch-clamp technique [15] was used in the cell-attached and excised inside-out configurations. Patch pipettes were made from borosilicate glass capillaries (GB 150T-8P, Science Products, Hofheim, Germany) on a horizontal Flaming/Brown micropipette puller (model P 97, Sutter Instruments, San Francisco, Calif., USA) in a three-step process and coated with Sylgard (Dow Corning, Midland, USA). Filled with physiological pipette solution, tip resistance was 3–5 M $\Omega$ . Seal resistances were 5–20 G $\Omega$ . Recordings were made with a BioLogic RK 300 amplifier (Science Products, Hofheim, Germany), whereby a steady holding potential was applied to the inside of the electrode.

### Solutions

Bath and physiological pipette solution contained (in mM): NaCl, 140; KCl, 2.5;  $CaCl_2$ , 0.5; 4-(2-hydroxyethyl)-1-piperazineethanesulphonic acid (HEPES)-NaOH buffer, 5 (pH 7.4). For pipette solutions with higher than physiological  $[K^+]$ ,  $K^+$  partially replaced  $Na^+$ . For low- $Cl^-$  solution, 130 mM  $Cl^-$  was replaced by equimolar  $CH_3SO_3^-$ . For low-cation solution, 100 mM  $Na^+$  was replaced by *N*-methyl-D-glucamine (NMDG<sup>+</sup>).  $Cs^+/Ba^{2+}$  solution contained (mM): CsCl, 140;  $BaCl_2$ , 2;  $CaCl_2$ , 0.5, HEPES-NaOH buffer, 5 (pH 7.4). Tetraethylammonium (TEA<sup>+</sup>) solution contained (in mM): TEA-Cl, 140;  $CaCl_2$ , 0.5; HEPES-NaOH buffer, 5 (pH 7.4). Tetrodotoxin (TTX, 1  $\mu$ M, Sigma) was present in all solutions. Experiments were carried out at room temperature (18–24 °C).

### Data processing

Recordings were digitized with a sampling frequency of 4 kHz and stored on the hard disk of an IBM-compatible computer. A 4-pole Bessel low-pass filter with a cut-off frequency of 1 kHz (unless otherwise mentioned) was used offline. Unitary current amplitudes were determined by fitting Gaussian curves to histograms of data points. For the analysis of open probability ( $P_o$ ) and dwell-time distributions channel openings were detected by setting a threshold midway between open and closed level either by hand or by a program which finds the threshold as the value which is both a minimum between two maxima in the amplitude histogram and the point of maximal change of current with time.  $P_o$  was then calculated as number of data points beyond this threshold relative to the total number of data points in at least three recording periods of 10 s. Dwell-times in periods of recording from one patch were binned in a histogram. The weighted sum of up to three exponential components was fitted to this distribution by a Levenberg-Marquardt algorithm.

Numerical values are given as means $\pm$ SEM. Whenever the frequency of occurrence of a channel type is given, the confidence interval based on an error probability of 0.05 is indicated. The significance of differences in occurrence of a channel type between groups was analysed with Fisher's exact probability test.

## Results

Ion channels were characterized and identified according to the following properties: ion selectivity, unitary conductance and kinetic parameters. Unless otherwise mentioned, graphic representations of these were based on data combined from WT and ADR mice of different ag-

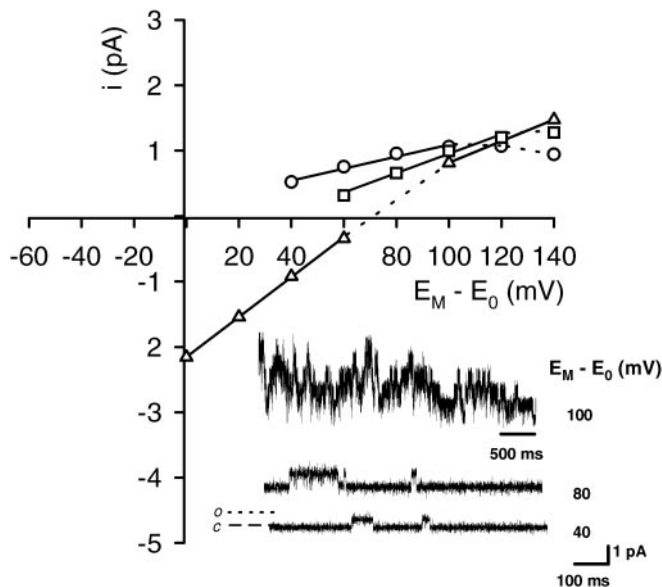


**Fig. 1** Delayed-rectifier  $K^+$  channel ( $K_{DR}$ ): unitary conductance and ion selectivity. Single-channel current/voltage ( $I/V$ ) relations as a function of pipette  $[K^+]_o$  ( $[K^+]_o$ ) in representative cell-attached patch-clamp recordings from isolated fibres from the interosseus muscle. The holding potential  $E_M - E_0$  (where  $E_M$  is the membrane potential and  $E_0$  the resting membrane potential, RMP) is equivalent to the deviation from RMP and is expressed conventionally, i.e. inside relative to outside. Negative currents are equivalent to flow of cations into or anions out of the cell. With 2.5 mM  $[K^+]_o$  (circles) the regression line fitting the linear part of the curve has a slope of 9.2 pS; with 25 mM  $[K^+]_o$  (squares) 14.8 pS and with 140 mM  $[K^+]_o$  (triangles) 16.5 pS. With 140 mM  $[K^+]_o$ , the slope conductance of the inwards current had to be determined by a different regression line and was 30.6 pS. The inset shows unitary currents recorded in the cell-attached configuration with 2.5 mM  $[K^+]_o$  at various holding potentials. Upper trace: directly after a voltage step from RMP to the indicated potential (c closed level, o open level)

es. For representations of channel abundance, data were processed separately according to developmental (age classes) and/or physiological status (myotonic, prior denervation).

#### Delayed-rectifier $K^+$ channels ( $K_{DR}$ )

There was almost never any channel activity at RMP in cell-attached patches from adult mouse interosseus muscle fibres when the pipette contained physiological saline. Stepping to a depolarizing pipette potential elicited single, often superposed, outwards currents in most recordings (Fig. 1). Within a few seconds the channels inactivated to a low steady-state ensemble open probability ( $NP_o$ , where  $N$  is the total number of channels) of about 0.05 at strongly depolarizing and 0.02 at moderately depolarizing holding potentials. The unitary conductance determined from the linear part of the current/voltage ( $I/V$ ) relation was  $10.6 \pm 0.3$  pS ( $n=37$ ), with slight inwards rectification at holding potentials higher than 100 mV. These characteristics are typical of  $K_{DR}$  chan-

nels [16, 31]. A-type  $K^+$  channels might contribute to the activity directly after voltage steps, but are probably not relevant for analyses of channel openings at steady-state voltages.

To test the  $K^+$  selectivity and to determine if  $K_{DR}$  channels also show activity at RMP, we raised the pipette  $[K^+]_o$  ( $[K^+]_o$ ). This shifted the current reversal potential, extrapolated from the linear part of the  $I/V$  relations, towards depolarizing membrane potentials. Fitting a straight line to the relationship between the reversal potentials and the logarithm of the pipette  $[K^+]_o$  yielded a 55 mV shift of reversal potential per tenfold shift in  $[K^+]_o$  ( $n=37$  for 2.5 mM  $[K^+]_o$ ,  $n=3$  for 25 mM  $[K^+]_o$  and  $n=3$  for 140 mM  $[K^+]_o$ ). This value is very close to the 58 mV predicted by the Nernst equation for a current carried exclusively by  $K^+$ . With 140 mM  $[K^+]_o$ , not only outwards but also inwards currents through  $K_{DR}$  channels could be recorded. These were characterized by noisy, sublevel-rich open states, especially at holding potentials close to the activation threshold of the channel, which is in the range of the RMP (c.f. the model in [6]).

In recordings with  $Cs^+/Ba^{2+}$  pipette solution  $K_{DR}$  had a unitary conductance of  $19.6 \pm 0.2$  pA ( $n=3$ ) and a zero-current potential of  $31.7 \pm 3.3$  mV ( $n=3$ ), consistent with previous reports showing considerable  $Cs^+$  permeability and only low blocking efficiency of  $Ba^{2+}$  on  $K_{DR}$  [20, 34].

Activity of  $K_{DR}$  could be observed in 107 out of 109 recordings from WT, in 19 out of 20 recordings from denervated WT and in all 106 recordings from ADR. There was thus no difference between the groups. Likewise,  $K_{DR}$  occurred with high frequency in recordings from young (23 out of 24 recordings from WT aged 15 days or less) as well as from adult mice (36 out of 37 recordings from WT aged 40 days or more).

#### Inwards-rectifying $K^+$ channels ( $K_{IR}$ )

With pipette  $[K^+]_o$  above physiological levels, inwards currents with long-lasting openings and low open-state noise, typical of  $K_{IR}$  channels [17, 23, 28], could be observed in several cell-attached recordings (Fig. 2). No outwards currents were discernible at potentials positive to the extrapolated reversal potential of the current. Occasionally, sublevels at about 2/3 of the unit amplitude were detected. Patch excision did not lead to further activation, indicating that this channel type is probably not regulated by ATP or  $Ca^{2+}$ . The channel was never detected with  $Cs^+/Ba^{2+}$  pipette solution ( $n=6$ ) [24].  $I/V$  relations were determined for different  $[K^+]_o$  and showed linearity in the range from a holding potential of  $-100$  mV to values near the zero-current potential. With 140 mM  $[K^+]_o$  the slope conductance of the channel averaged  $31.1 \pm 1.4$  pS ( $n=11$ ). The zero-current potential shift for a tenfold change in  $[K^+]_o$  was 40 mV ( $n=15$  for 25 mM  $[K^+]_o$ ,  $n=6$  for 40 mM  $[K^+]_o$  and  $n=11$  for 140 mM  $[K^+]_o$ ). This value indicates that the current is mainly, but not solely, carried by  $K^+$ ; alternatively deviations from

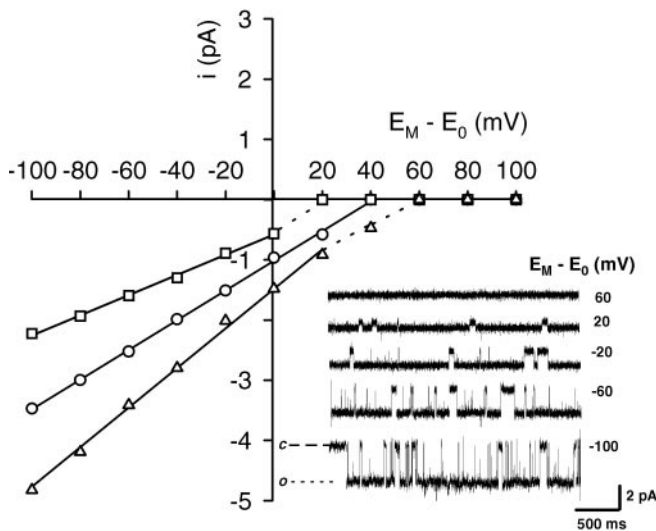


**Fig. 2** Inwards-rectifying  $K^+$  channel ( $K_{IR}$ ): unitary conductance and ion selectivity. Unitary  $I/V$  relations as a function of  $[K^+]_o$  in representative cell-attached recordings from isolated interosseus fibres. With 25 mM  $[K^+]_o$  (squares) the regression line fitting the  $I/V$  curve has a slope of 16.8 pS; with 40 mM  $[K^+]_o$  (circles) 24.6 pS and with 140 mM  $[K^+]_o$  (triangles) the linear part of the curve has a slope of 32.8 pS. The inset shows unitary currents recorded in the cell-attached configuration with 140 mM  $[K^+]_o$  at various holding potentials

linearity might be caused by saturation effects at high  $[K^+]_o$ .

The unitary conductance of  $K_{IR}$  is dependent on  $[K^+]_o$  and is described by an exponential function [28]:  $\gamma = C \cdot [K^+]_o^b$ , where  $\gamma$  is the unitary conductance and  $C$  and  $b$  are constants. Determination of the function parameters by a double-logarithmic plot of the conductance against  $[K^+]_o$  yielded 4.1 for  $C$  and 0.42 for  $b$ . This roughly square-root dependence has also been observed for the anomalously rectifying whole cell current [14] and for other native and cloned  $K_{IR}$  channels [21, 28, 38].

Since we were interested in the contribution of  $K_{IR}$  to resting  $G_K$  under physiological conditions, we not only recorded with high- $[K^+]$  pipette solution which is, although very unphysiological, commonly used to study  $K_{IR}$ , but also with 25 mM  $[K^+]$  pipette solution. Both  $P_o$  and kinetic parameters depended on the pipette solution used. This dependence is not directly due to the change in  $[K^+]_o$ , but to a voltage-dependent block by  $Na^+$  [23]. With 25 mM  $[K^+]$  solution,  $P_o$  declined markedly upon changing from a slightly negative pipette potential to strongly hyperpolarizing potentials (Fig. 3A), caused by a voltage dependence of dwell-times: The mean open time, obtained by fitting a single exponential function to the open-time distributions, declined from 40 ms at  $-20$  mV holding potential to about one-tenth of this value at  $-100$  mV (Fig. 3B). Additionally, the time constant ( $\tau_c$ ) for brief channel closures, gained by fitting the weighted sum of two exponentials to closed-time histograms, increased slightly with hyperpolarization (data not shown).

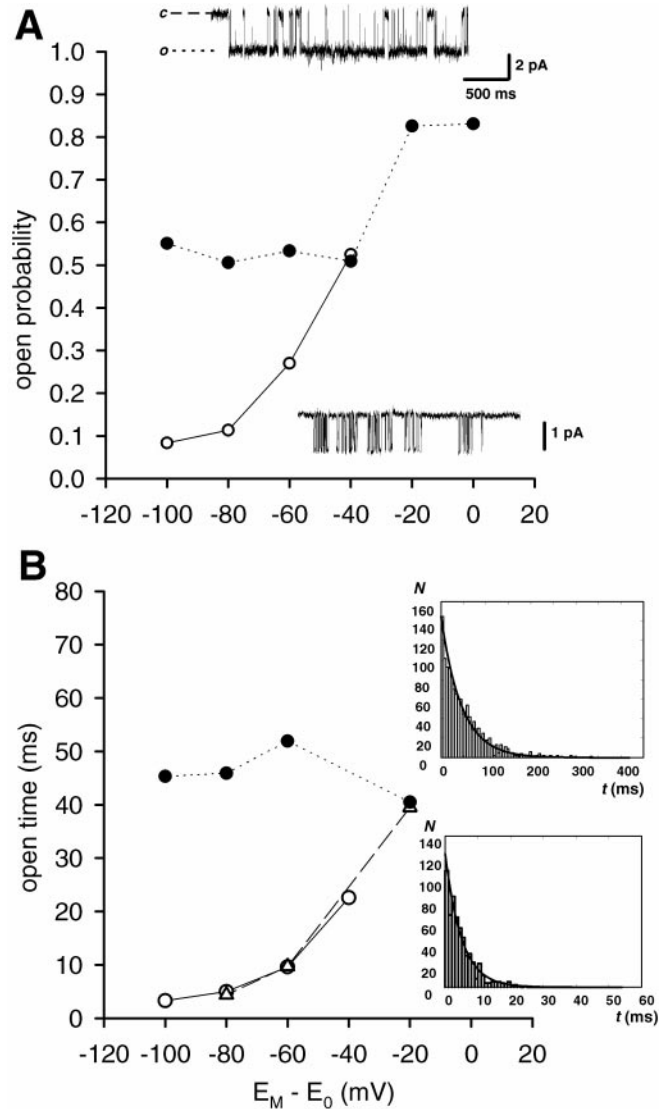


**Fig. 3A, B**  $K_{IR}$ : open state probability and mean open times. **A** The open probability of single  $K_{IR}$  channels in cell-attached recordings with 140 mM (solid circles) or 25 mM (open circles)  $[K^+]_o$  is shown as a function of holding potential. The upper inset shows a unitary current trace recorded cell-attached with 140 mM  $[K^+]_o$  at  $-100$  mV holding potential. The current trace in the lower inset was recorded at the same holding potential but with 25 mM  $[K^+]_o$  (filter 500 Hz). **B** Mean open times as a function of holding potential. Recordings with 25 mM (open symbols) and with 140 mM (solid circles)  $[K^+]_o$ . Data from the same recordings as in **A** (open and solid circles) and from a different recording (triangles). The upper inset shows an open time histogram based on a recording with 140 mM  $[K^+]_o$  at  $-80$  mV holding potential containing 1326 channel openings. The histogram is fitted by a one-parameter exponential function with an open time constant  $\tau_o$  of 45.9 ms. The open time histogram in the lower inset is constructed from periods of cell-attached recording with 25 mM  $[K^+]_o$  at the same holding potential and contains 616 channel openings (filter 500 Hz). The exponential fit yields a  $\tau_o$  of 5.0 ms

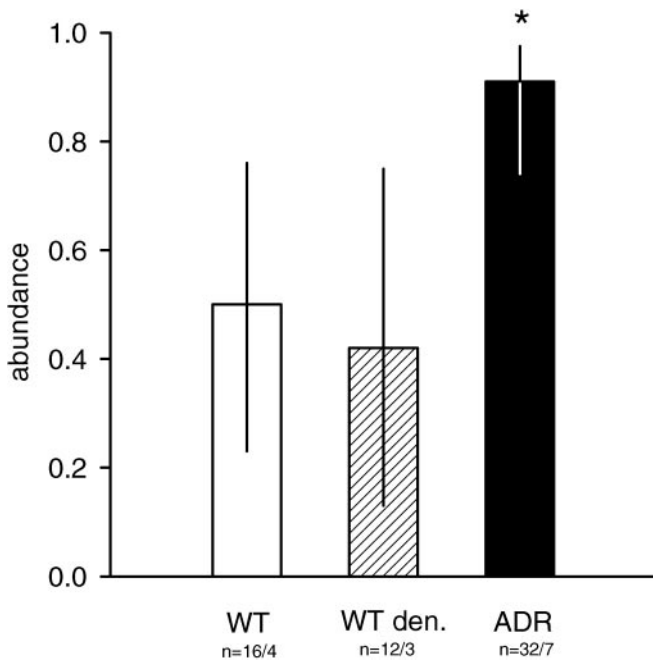


**Fig. 4**  $K_{IR}$ : abundance in wild-type (WT), denervated (*den*) and myotonic (mutant “arrested development of righting response”, *ADR*) mouse interosseus muscle fibres. Frequency of occurrence of  $K_{IR}$  activity in cell-attached recordings from WT, WT *den* (fibres isolated 7 days post-operative) and ADR fibres. The bars represent confidence intervals based on an error probability of 0.05. Sample sizes are given as *n* recordings/animals. \* $P < 0.01$  vs. WT (Fisher test)

In contrast, recording  $K_{IR}$  with 140 mM  $[K^+]_o$  led to high  $P_o$ , even at strongly hyperpolarizing holding potentials (Fig. 3A). This was consistent with the dwell-time analysis since neither the mean open-time (Fig. 3B) nor the closed-time components (data not shown) showed significant voltage dependence.

$K_{IR}$  channels occurred more frequently in recordings from ADR fibres than in WT fibres (Fig. 4). Whereas in WT preparations this type of channel was active in 50% of the cell-attached patches, it could be observed in 91% of recordings from ADR muscle cells ( $P < 0.01$ , Fisher test). For this comparison we pooled data from mice of different ages, but the age distribution was similar for the compared groups (WT: range 29–95 days, mean 67.4 days; ADR: range 28–98 days, mean 58.2 days). An unequal age distribution would have been critical, because the inwards-rectifying  $K^+$  whole-cell current is up-regulated during development [12]. Since the current reaches a plateau phase at about postnatal day 20, we only included animals older than this in our analyses. If there was an influence of developmental up-regulation, the difference between the groups should have been the reverse of that observed, since the mean age in the ADR group is lower than the corresponding value for the WT group. No influence of denervation on the occurrence of  $K_{IR}$  could be observed (Fig. 4).

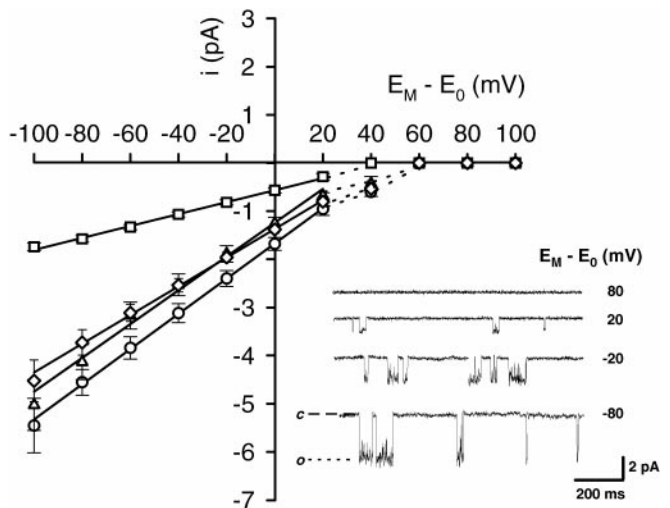


**Fig. 5** Inwards-rectifying cation channel ( $C_{IR}$ ): unitary conductance and ion selectivity. Cell-attached  $I/V$  relations in recordings from isolated interosseus fibres with physiological (circles,  $n=12$ ), low-chloride (triangles,  $n=6$ ), low-cation (squares,  $n=11$ ) and  $Cs^+/Ba^{2+}$  (diamonds,  $n=6$ ) pipette solution. The inset shows unitary currents recorded in the cell-attached configuration with physiological pipette solution at various holding potentials (filter 500 Hz)

#### Inwards-rectifying cation channel ( $C_{IR}$ )

In less than 30 day-old mice a novel channel activity could be observed frequently in cell-attached recordings from interosseus fibres near RMP and at hyperpolarizing holding potentials when the patch pipette contained physiological saline (Fig. 5). This channel showed intervals of fast open-closed transitions that were separated by long closed periods, leading to a bursting characteristic. Due to inadequate resolution of open-closed transitions or to subconductance states, the open state of the channel was much noisier than the closed state. Upon excision of the membrane patch this channel activity disappeared, indicating regulation by intracellular factors or interaction with the cytoskeleton. No outwards currents could be recorded, although in most recordings, solution conditions were symmetrical for the cations for which the channel was permeable (see below). The channel can thus be characterized as inwards rectifying, and was therefore termed  $C_{IR}$ . With physiological saline as pipette solution, the slope conductance of the linear part of the  $I/V$  curve averaged  $36.0 \pm 1.6$  pS ( $n=20$ ) and  $32.9 \pm 1.0$  pS ( $n=14$ ) for WT and ADR muscle fibres respectively.

Increasing the pipette  $[K^+]$  to 25 mM or 140 mM by replacing equimolar amounts of  $Na^+$  changed neither the zero-current potential nor the unitary conductance significantly (data not shown), thus indicating that  $C_{IR}$  is not  $K^+$  selective. To test the permeability for  $Cl^-$  we replaced all but 13.5 mM  $Cl^-$  in the pipette solution by methanesulphonate. A very slight shift of the zero-current potential in a direction opposite to that expected for  $Cl^-$  channels and no change in unitary conductance was observed (Fig. 5). On the other hand, replacing about 2/3 of the cat-

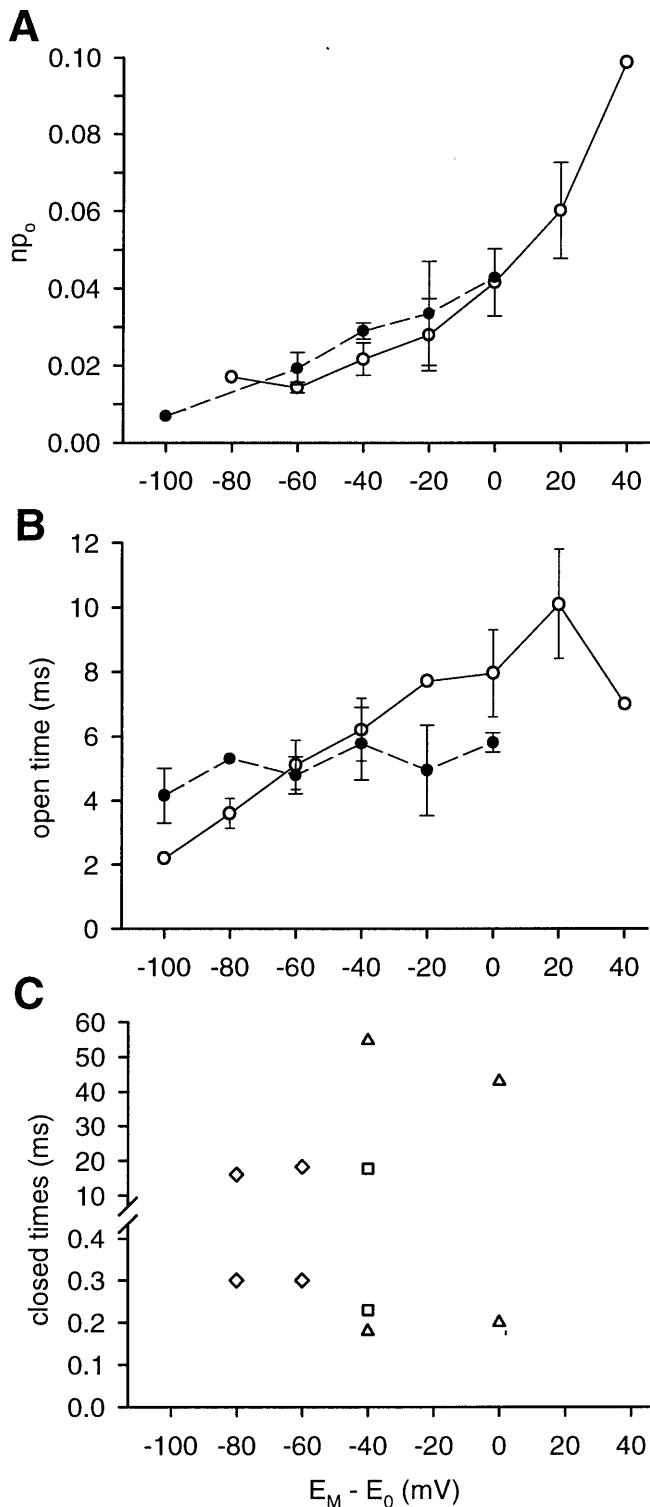
ions in the pipette solution by NMDG<sup>+</sup> shifted the zero-current potential from  $47.3 \pm 2.5$  ( $n=20$ ) to  $35.5 \pm 3.7$  mV ( $n=11$ ) and reduced the unitary conductance to  $13.0 \pm 0.6$  pS ( $n=11$ ), indicating that  $C_{IR}$  is a cation channel.  $C_{IR}$  turned out to be impermeable to tetraethylammonium ions, since no channel openings could be observed in 12 recordings with 140 mM TEA<sup>+</sup> solution from 14- to

28-day-old WT mice, an age group in which the channel is abundant in recordings with other pipette solutions ( $P < 0.001$  vs. 29- to 30-day WT, Fisher test). Partial replacement of cations by TEA<sup>+</sup> led to effects similar to replacement by NMDG<sup>+</sup> (data not shown), indicating that, whilst  $C_{IR}$  is not permeable for TEA<sup>+</sup>, it is not blocked by the latter. In recordings with Cs<sup>+</sup>/Ba<sup>2+</sup> pipette solution  $C_{IR}$  had a conductance of  $28.9 \pm 2.1$  pS ( $n=6$ ) and a zero-current potential of  $47.5 \pm 2.5$  mV ( $n=6$ ). This demonstrates that  $C_{IR}$  is not blocked by Ba<sup>2+</sup> and that it is nearly as permeable to Cs<sup>+</sup> as to Na<sup>+</sup> and K<sup>+</sup> (Fig. 5).

The  $NP_o$  for  $C_{IR}$  is low and voltage dependent, with values between 0.01 and 0.02 at strongly hyperpolarizing holding potentials, and about 5 times higher at depolarizing potentials (Fig. 6A). Distributions of open times were fitted by one exponential. At least for WT the mean open time was, like  $NP_o$ , dependent on holding potential, with longer open times at positive holding potentials (Fig. 6B). For closed times, a fit by the weighted sum of two exponentials was necessary. The smaller  $\tau$  value seemed to be independent of voltage, while the higher value varied between recordings and is therefore difficult to interpret (Fig. 6C).

The percentage of cell-attached patches showing  $C_{IR}$  activity was dependent on age (Fig. 7). Whereas in recordings from 10- to 14-day-old WT mice the channel was always present, it was only observed in 1 out of 28 recordings from mice older than 60 days ( $P < 0.001$ , Fisher test). For ADR, the developmental change resembles that of WT, although the channel occurred slightly more often in recordings from older ADR mice than in WT (not significant).

We tested if neural excitation of the muscle cell is the regulating factor for  $C_{IR}$  abundance by denervating the muscles of one leg 6–8 days prior to recording. As  $C_{IR}$  activity was not found in 20 recordings from denervated muscle, we conclude that it is not up-regulated by this condition.



#### Rare channel activities

In cell-attached recordings with higher than physiological [K<sup>+</sup>] in the pipette solution, inwards currents of a channel type with fast open-closed transitions, grouped in bursts, were seen in 3 out of 21 recordings from WT

**Fig. 6A–C**  $C_{IR}$ : open state probability and dwell-times in WT and ADR fibres. **A** Ensemble open probability ( $NP_o$ ) in cell-attached recordings with physiological pipette solution as a function of holding potential. *Open symbols*: WT ( $n=1-4$ ); *solid symbols*: ADR ( $n=1-3$ ). **B** Mean open times, determined by fitting single exponential functions to open time histograms obtained from cell-attached recordings with physiological pipette solution (filter 500 Hz), as a function of holding potential. *Open symbols*: WT ( $n=1-4$ ); *solid symbols*: ADR ( $n=1-4$ ). **C** Mean closed times, determined by fitting two exponential functions to closed time histograms from cell-attached recordings with physiological pipette solution, as a function of holding potential. Different recordings are represented by different symbols; WT only

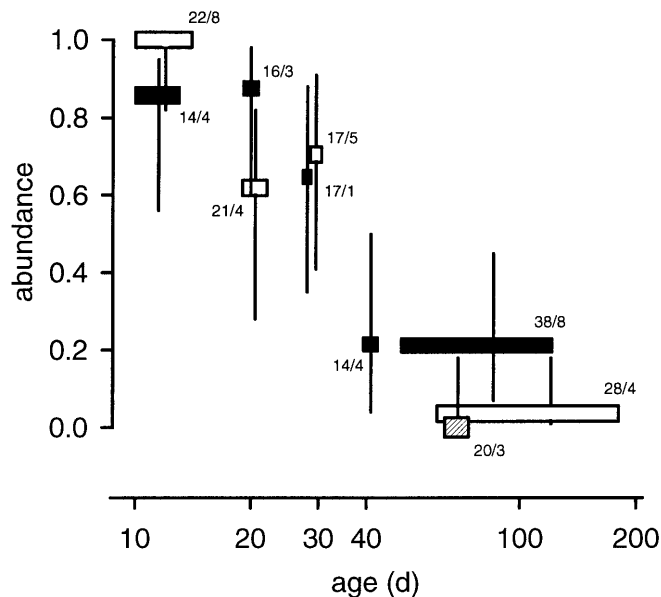


**Fig. 7**  $C_{IR}$ : abundance as a function of age and influence of myotonia and denervation. Frequency of occurrence of  $C_{IR}$  activity in cell-attached recordings from interosseus fibres. The box width shows the age range of individual classes (logarithmic scale). Vertical bars represent the confidence intervals based on an error probability of 0.05. Sample sizes are given as number of recordings/number of preparations. Open symbols: WT; solid symbols: ADR; hatched symbol: denervated muscle (fibres isolated 7 days post-operative)

and only in 1 out of 36 recordings from ADR fibres. In the cell-attached conformation with 25 mM  $[K^+]_o$  the channel had a conductance of  $19.4 \pm 1.3$  pS ( $n=2$ ) and a zero-current potential identical to that of  $K_{DR}$  and  $K_{IR}$ . Activation of this type of channel often could be observed following excision of the membrane patch. The kinetic characteristics, analysed in the inside-out conformation (open-time  $\tau_o$  0.9 ms at a membrane potential of  $-80$  mV increasing to 2.0 ms at 20 mV; a long closed time  $\tau_{c1}$  of 12.9 ms at  $-80$  mV decreasing to 0.7 ms at 20 mV and a brief voltage-independent closed time  $\tau_{c2}$  of about 0.3 ms; data not shown), are in good agreement with those of ATP-sensitive  $K^+$  channels ( $K_{ATP}$ ) [30]. To our knowledge, the only other channels that might have comparable kinetics are  $Ca^{2+}$ -dependent  $K^+$  channels ( $K_{Ca}$ ). Since, however, these are active in another voltage range, we assume that the recorded channels are  $K_{ATP}$  channels.

Upon strong depolarization of the cell membrane, outwards currents of a channel with a conductance of  $54.9 \pm 6.1$  pS ( $n=5$ ) in cell-attached patches with physiological pipette solution could be recorded sporadically (data not shown). Since channels of this type could be activated by the addition of the ryanodine receptor agonist caffeine, which causes the release of  $Ca^{2+}$  from internal stores, we conclude that these are  $K_{Ca}$  channels [2]. The data were not sufficient to allow for a comparison of abundance between WT and ADR or denervated and control muscles.

## Discussion

### General considerations

The aim of this study was to identify  $K^+$ -permeable ion channels that contribute to resting  $G_K$  as shown by their activity near RMP in intact, native muscle fibres and that are regulated by muscle fibre maturation and the pattern of muscle activity. While a lack of excitation was established by denervation of WT muscle, the myotonic ADR mouse served as a model for hyperexcitability. It should be kept in mind that the loss-of-function mutation that inactivates the muscular  $Cl^-$  channel  $ClC-1$  in myotonic ADR mice [13, 32] has a highly specific primary effect, but secondarily affects the expression of a number of genes, including some coding for other ion channels [18, 36]. While cell-attached recording is as close to the situation in the animal as technically possible, it should be noted that isolation (and therefore denervation) of the fibres per se may induce physiological changes. However, previous work has shown that the effects of myotonia and prior denervation persist for several days in isolated fibres [25].

### Characteristics and identification of ion channels

We recorded a cation channel,  $C_{IR}$ , with single-channel characteristics different from any previously described ion channel. With respect to conductance and kinetics,  $C_{IR}$  resembles mechanosensitive cation channels, a low resting activity of which has been demonstrated in muscle fibres of young mice [11]. Systematic application of pressure was not possible with our recording equipment, but there was no indication of sensitivity to membrane deformation. Furthermore, whereas  $C_{IR}$  rectifies inwardly, the mechanosensitive channels show outwards currents with a high open probability [10]. Low abundance in adult muscle, low open probability and rundown upon patch excision may explain why  $C_{IR}$  has not been recorded in previous studies on native mammalian muscle fibres [4, 8, 16].

In contrast, two kinds of  $K^+$ -selective ion channels active at RMP,  $K_{DR}$  and  $K_{IR}$ , could be identified unambiguously, based on the analysis of single-channel properties as outlined in Results. According to RNA hybridization data at least two  $K_{IR}$  channel types are expressed in skeletal muscle:  $K_{IR2.1}$  (IRK1) and  $K_{IR2.2}$  (IRK2) [33]. We cannot decide which one of these two is the  $K_{IR}$  channel recorded in the present study, because changes in conductance and kinetics due to different expression systems seem to be larger than the differences between the channel types per se (c.f. [26, 33]). Further studies on native systems like the interosseus muscle preparation are needed to correlate the abundance of ion channels with mRNA levels in the same cell, thus bridging the gap between information at the nucleic acid level and the level of single channels in an excitable cell.

## Contribution of cation channels to resting $G_K$

Although  $K_{DR}$  channels were present in nearly every cell-attached recording, the following argument suggests that they contribute only a small fraction to resting  $G_K$ . Steady-state  $NP_o$  for  $K_{DR}$  near RMP was 0.02 at the most. The contribution of  $K_{DR}$  to the macroscopic sarcolemmal  $G_K$  can be calculated according to  $G = N \cdot P_o \cdot \gamma \cdot A^{-1}$  (where  $A$  is the area of the membrane patch). Since, in contrast to our protocol, membrane conductances are usually measured at 37 °C [7, 19], so that  $K_{DR}$  unitary conductance must be corrected by a  $Q_{10}$  value of 1.45 [20], yielding approximately 19 pS. Assuming a patch membrane area of about 5  $\mu\text{m}^2$  for 3- to 5-M $\Omega$  pipettes [27],  $K_{DR}$  would contribute 8  $\mu\text{S cm}^{-2}$  or less to total  $G_K$ , for which a value of 369  $\mu\text{S cm}^{-2}$  for extensor digitorum longus (EDL) muscle fibres [19] has been reported. For the sternocostalis muscle about 260  $\mu\text{S cm}^{-2}$  and 100  $\mu\text{S cm}^{-2}$  have been determined for fibres of WT and ADR mice respectively [7].  $K_{DR}$  single-channel activity has been observed previously in intact interosseus fibres at steady-state voltages near RMP and it has been suggested that  $K_{DR}$  is responsible for resting  $G_K$  [4]. However, in view of the above calculation, we conclude that  $K_{DR}$  can contribute 3–8 % at the most to the resting  $G_K$  of normal and myotonic muscle fibres, respectively.

In contrast to  $K_{DR}$ ,  $K_{IR}$  channels show a high open probability at steady-state voltages near RMP. Thus it is tempting to propose  $K_{IR}$  as a channel type being responsible for a substantial fraction of resting  $G_K$ . However, estimating the contribution of  $K_{IR}$  to resting  $G_K$  is complicated by the fact that  $K_{IR}$  single-channel currents are difficult to measure under physiological conditions. Based on recordings with three different, higher than physiological  $[K^+]_o$ , we determined the dependence of  $K_{IR}$  unitary conductance on  $[K^+]_o$  to be  $\gamma = 4.1 \cdot [K^+]_o^{0.42}$ , leading to an extrapolated conductance of 6 pS in 2.5 mM  $[K^+]_o$ . Given the temperature dependence of  $K_{IR}$  ( $Q_{10}$  of 1.7, [28]), the unitary conductance at 37 °C is 13 pS. Since not only the unitary conductance but also the open probability of  $K_{IR}$  is influenced by the extracellular solution conditions, a  $P_o$  of 0.5 under physiological conditions might be a reasonable estimate. Since only the frequency of occurrence of  $K_{IR}$  activity, regardless of the number of channels, was determined, the mean number of channels per membrane patch must be calculated from this frequency, assuming random distribution in the sarcolemma. This yields means of 0.7 and 2.3 channels per membrane patch for WT and ADR fibres, respectively. Thus, in muscle fibres of WT mice, about 90  $\mu\text{S cm}^{-2}$ , equivalent to one-third of  $G_K$ , can be attributed to  $K_{IR}$ , which is in the range of values estimated for heart muscle cells [28].

The newly described cation channel  $C_{IR}$  is abundant in interosseus fibres of young mice but shows only a low open probability. Estimating the contribution of  $C_{IR}$  to resting  $G_K$  without taking into account a temperature effect results in values 50  $\mu\text{S cm}^{-2}$  or less. Since, at least in the rat,  $G_K$  is higher in muscle fibres of young than in

those of adult animals (826  $\mu\text{S cm}^{-2}$  for 12- to 14-day vs. 308  $\mu\text{S cm}^{-2}$  for 70- to 80-day postnatal in EDL fibres [9]), only about 6% of  $G_K$  can be attributed to  $C_{IR}$  in young mice.

$K_{ATP}$  and  $K_{Ca}$  channels were only sporadically active in our cell-attached recordings, and seem therefore not to be relevant for intact fibres at rest under physiological conditions. This is in contrast to recordings from membrane patches *excised* from skeletal muscle fibres [1, 39]. Our results are in accordance with the finding that  $K_{Ca}$  does not play a major role for resting  $G_K$  in muscle fibres of adult (but not aged) rats [35].

## Influence of maturation and myotonia on cation channel abundance

Whereas  $K_{DR}$  channels are abundant in the sarcolemma of interosseus fibres, regardless of age and pattern of muscle activity,  $K_{IR}$  could be recorded more frequently in membrane patches from myotonic ADR than in those from WT fibres. This is surprising, since sarcolemmal  $G_K$  is reduced in the ADR mouse [7]. In addition, down-regulation following denervation could not be observed in our study, in contrast to whole-cell recordings of  $K_{IR}$  [12]. Furthermore, the reported effect of denervation on the  $K_{IR}$  whole-cell current [12] does not parallel the change in  $G_K$  which, at least in the rat, increases following denervation [5]. These discrepancies cast doubt on the putative role of  $K_{IR}$  for resting  $G_K$  in muscle cells.

The abundance of the hitherto undescribed cation channel  $C_{IR}$  decreases during muscle maturation. However, muscle activity seems not to be the regulating factor for this change because neither hyperexcitability nor denervation influences its abundance.

In conclusion, a substantial fraction of sarcolemmal  $G_K$  in mammalian skeletal muscle at rest seems to be due to  $K_{IR}$ , whereas the contribution of  $K_{DR}$  is only minor, and  $C_{IR}$  contributes to  $G_K$  only in immature muscle. Surprisingly,  $K_{IR}$  single-channel abundance is higher in myotonic ADR than in WT mice, whereas total  $G_K$  is lower. The sum of the estimated contributions to resting  $G_K$  of all channel types that we could detect in the sarcolemma accounts for only about one-half of the resting  $G_K$  reported for WT. Thus it is possible that further  $K^+$ -permeable ion channels escaped our single-channel analysis, due to their location in t-tubular membranes, or extremely long open times or to extremely small unitary currents.

**Acknowledgements** This work was supported by the German Research Council (DFG, SFB 223). We thank Drs. D. Conte-Camerino and D. Tricarico (Bari), E. Wischmeyer (Göttingen), and M.-F. Chen (Bielefeld) for helpful discussions.

## References

- Allard B, Rougier O (1997) Similarity of ATP-dependent K<sup>+</sup> channels in skeletal muscle fibres from normal and mutant *mdx* mice. *J Physiol (Lond)* 498:319–325
- Blatz AL, Magleby KL (1987) Calcium-activated potassium channels. *Trends Neurosci* 10: 463–467
- Breitwieser GE (1996) Mechanisms of K<sup>+</sup> channel regulation. *J Membr Biol* 152:1–11
- Brinkmeier H, Zachar E, Rüdell R (1991) Voltage-dependent K<sup>+</sup> channels in the sarcolemma of mouse skeletal muscle. *Pflügers Arch* 419:486–491
- Camerino D, Bryant SH (1976) Effects of denervation and colchicine treatment on the chloride conductance of rat skeletal muscle fibers. *J Neurobiol* 7:221–228
- Chapman ML, VanDongen HMA, VanDongen AMJ (1997) Activation-dependent subconductance levels in the drk1 K channel suggest a subunit basis for permeation and gating. *Biophys J* 72:708–719
- Chen M-F, Niggeweg R, Iaizzo PA, Lehmann-Horn F, Jockusch H (1997) Chloride conductance in mouse muscle is subject to post-transcriptional compensation of the functional Cl<sup>-</sup> channel 1 gene dosage. *J Physiol (Lond)* 504:75–81
- Chua M, Betz WJ (1991) Characterization of ion channels on the surface membrane of adult rat skeletal muscle. *Biophys J* 59:1251–1260
- Conte Camerino D, De Luca A, Mambrini M, Vrbová G (1989) Membrane ionic conductance in normal and denervated skeletal muscle of the rat during development. *Pflügers Arch* 413:568–570
- Franco A, Lansmann JB (1990) Stretch-sensitive channels in developing muscle cells from a mouse cell line. *J Physiol (Lond)* 427:361–380
- Franco-Obregón A, Lansmann JB (1994) Mechanosensitive ion channels in skeletal muscle from normal and dystrophic mice. *J Physiol (Lond)* 481:299–309
- Gonoi T, Hasegawa S (1991) Postnatal induction and neural regulation of inward rectifiers in mouse skeletal muscle. *Pflügers Arch* 418:601–607
- Gronemeier M, Condie A, Prosser J, Steinmeyer K, Jentsch TJ, Jockusch H (1994) Nonsense and missense mutations in the muscular chloride channel gene *Clc-1* of myotonic mice. *J Biol Chem* 269:5963–5967
- Hagiwara S, Takahashi K (1974) The anomalous rectification and cation selectivity of the membrane of a starfish egg cell. *J Membr Biol* 18:61–80
- Hamill OP, Marty A, Neher E, Sakmann B, Sigworth FJ (1981) Improved patch-clamp techniques for high-resolution current recording from cells and cell-free membrane patches. *Pflügers Arch* 391:85–100
- Hochermann SD, Bezanilla F (1996) A patch-clamp study of delayed rectifier currents in skeletal muscle of control and *mdx* mice. *J Physiol (Lond)* 493:113–128
- Isomoto S, Kondo C, Kurachi Y (1997) Inwardly rectifying potassium channels: their molecular heterogeneity and function. *Jpn J Physiol* 47:11–39
- Jockusch H (1990) Muscle fibre transformations in myotonic mutants. In: Pette D (ed) *The dynamic state of muscle fibers*. de Gruyter, Berlin, pp 429–443
- Kerr LM, Sperelakis N (1983) Effects of pH on membrane resistance in normal and dystrophic mouse skeletal muscle fibers. *Exp Neurol* 82:203–214
- Koh DS, Vogel W (1996) Single-channel analysis of a delayed rectifier K<sup>+</sup> channel in *Xenopus* myelinated nerve. *J Membr Biol* 149: 221–232
- Kubo Y, Baldwin TJ, Jan YN, Jan LY (1993) Primary structure and functional expression of a mouse inward rectifier potassium channel. *Nature* 362:127–133
- Kurtz R, Schirm T, Jockusch H (1998) Regulation by muscle activity of cation channels. A patch clamp study on isolated interosseus fibres (abstract). *Pflügers Arch* 435 [suppl]:R179
- Matsuda H, Stanfield PR (1989) Single inwardly rectifying potassium channels in cultured muscle cells from rat and mouse. *J Physiol (Lond)* 414:111–124
- Matsuda H, Matsuura H, Noma A (1989) Triple-barrel structure of inwardly rectifying K<sup>+</sup> channels revealed by Cs<sup>+</sup> and Rb<sup>+</sup> block in guinea-pig heart cells. *J Physiol (Lond)* 413:139–157
- Mehrke G, Brinkmeier H, Jockusch H (1988) The myotonic mouse mutant ADR: electrophysiology of the muscle fiber. *Muscle Nerve* 11:440–446
- Omori K, Oishi K, Matsuda H. (1997) Inwardly rectifying potassium channels expressed by gene transfection into the green monkey kidney cell line COS-1. *J Physiol (Lond)* 499:369–378
- Sakmann B, Neher E (1995) *Single channel recording*. Plenum, New York
- Sakmann B, Trube G (1984) Conductance properties of single inwardly rectifying potassium channels in ventricular cells from guinea-pig heart. *J Physiol (Lond)* 347:641–657
- Sedehizade F, Klocke R, Jockusch H (1997) Expression of nerve-regulated genes in muscles of mouse mutants affected by spinal muscular atrophies and muscular dystrophies. *Muscle Nerve* 20:186–194
- Spruce AE, Standen NB, Stanfield PR (1987) Studies of the unitary properties of adenosine-5'-triphosphate-regulated potassium channels of frog skeletal muscle. *J Physiol (Lond)* 382:213–236
- Standen NB, Stanfield PR, Ward TA (1985) Properties of single potassium channels in vesicles formed from sarcolemma of frog skeletal muscle. *J Physiol (Lond)* 364:339–358
- Steinmeyer K, Klocke R, Ortlund C, Gronemeier M, Jockusch H, Gründer S, Jentsch TJ (1991) Inactivation of muscle chloride channel by transposon insertion in myotonic mice. *Nature* 354:301–304
- Takahashi N, Morishige KI, Jahangir A, Yamada M, Findley I, Koyama H, Kurachi Y (1994) Molecular cloning and functional expression of cDNA encoding a second class of inward rectifier potassium channels in rat brain. *J Biol Chem* 269: 23274–23279
- Trequatrin C, Petris A, Franciolini F (1996) Characterization of a neuronal delayed rectifier K current permeant to Cs and blocked by verapamil. *J Membr Biol* 154:143–153
- Tricarico D, Petrucci R, Conte Camerino D (1997) Changes of the biophysical properties of calcium-activated potassium channels of rat skeletal muscle fibres during aging. *Pflügers Arch* 434:822–829
- Vullhorst D, Klocke R, Bartsch JW, Jockusch H (1998) Expression of the potassium channel KV3.4 in mouse skeletal muscle parallels fiber type maturation and depends on excitation pattern. *FEBS Lett* 421:259–262
- Wei A, Covarrubias M, Butler A, Baker K, Pak M, Salkoff L (1990) K<sup>+</sup> current diversity is produced by an extended gene family conserved in *Drosophila* and mouse. *Science* 248:599–603
- Wischmeyer E, Lentz K-U, Karschin A (1995) Physiological and molecular characterization of an IRK-type inward rectifier K<sup>+</sup> channel in a tumour mast cell line. *Pflügers Arch* 429: 809–819
- Woll KH, Lönnendonker U, Neumcke B (1989) ATP-sensitive potassium channels in adult mouse skeletal muscle: Different modes of blockage by internal cations, ATP and tolbutamide. *Pflügers Arch* 414:622–628